Journal of Theoretical and Applied Mechanics, Sofia, Vol.51 (2021) pp. 218-241

In memory of JORDAN G. BRANKOV

HIGH-TEMPERATURE EXPANSIONS FOR THE SPIN = 1 HEISENBERG MODEL: THE CASE OF THE HEXAGONAL FERRIMAGNET $RbNiF_3$

KIRIL A. KREZHOV*

Institute for Nuclear Research and Nuclear Energy and Institute of Electronics, Bulgarian Academy of Sciences, Tsarigradsko Chaussée 72, 1784 Sofia, Bulgaria

[Received: 22 March 2021. Accepted: 29 March 2021]

ABSTRACT: The high-temperature series in powers of reciprocal temperature up to sixth order for the magnetic susceptibility χ and up to fifth order for specific heat were determined for a three dimensional Heisenberg model of a hexagonal ferrimagnet with competing interactions (two different of opposite signs first neighbour exchange constants) and any spin value S. The scheme of spin-spin interactions is open, in the sense that the neighbors to whom a given site is coupled do not interact with each other. The power series were analysed by the method of optimal transformation of the variable. The study was carried out for the ratio of exchange constants $R = J_2/J_1$ in the interval $-3.0 \leq R \leq -0.2$ ($J_1 < 0$, $J_2 > 0$). The behaviour of the magnetic susceptibility and specific heat by taking into account the dominant coupling constants and the spin number $S = 1$ valid for $RbNiF_3$ is presented and compared with available theoretical and experimental results.

KEY WORDS: Series expansions, Quantum magnetism, Exchange interactions, Halide.

1 INTRODUCTION

To study the critical behavior of lattice systems, in the absence of accurate results, the method of high-temperature expansions of thermodynamic functions in a series of powers of the dimensionless ratio of the interaction couplings to temperature has been widely used since the sixties [1–4]. Systematic series expansions for statistical physics models defined on a lattice assure a profitable complement to renormalization group studies and numerical Monte Carlo simulations. In particular, it proved to be a generally applicable method to determine thermodynamic quantities for magnetic systems, including the frustrated ones. With the rapid improvement of computing resources over the last decade, both in speed and memory, great progress has been made in applying the method by developing advanced computer codes that allow a

*Corresponding author e-mail: kiril.krezhov@gmail.com

significant expansion of the order of the series, see e.g. [5]. The method is aimed at obtaining information about the features of thermodynamic functions at the phase transition point based on a finite number of accurately calculated coefficients in this series expansion [6–8]. In this case, it is inevitable to make some assumptions about the possible nature of the singularities of the studied functions and to apply special extrapolation techniques [9, 10].

The possibilities for extracting reliable physical information in the analysis of high-temperature series have been discussed in a number of studies, for example [4, 7], the review works [6, 8, 10] and the literature cited in them. The methods used to extract estimates of the critical parameters from the known expansion coefficients largely fall into two classes. One class is based on the ratio method, initially developed by Domb and Sykes [11], and modified and extended subsequently by many authors.

J.G. Brankov and the author of this article proposed and verified a new method for analysis of high-temperature series - a method for optimal transformation of the variable from the high-temperature series [12, 13] without prior knowledge of the locations of perturbing nonphysical singularities in the complex plane. The results obtained using this method in the analysis of constructed test functions, as well as known high-temperature series for magnetic susceptibility in the Heisenberg spin $S = 1/2$ model characterized by strongly irregular behavior for the three cubic cells (sc, bcc, fcc), have shown that it is possible to significantly reduce the influence of perturbing non-physical singularities. In the case of cubic cells by employing the method of optimal transformation, reliable estimates of the critical parameters were obtained even in the analysis of relatively short series consisting of only up to six terms. The results were comparable with the best estimates known from the literature. Moreover, the latter were obtained on the basis of an analysis of significantly longer series of nine-ten members.

In the present work, the application of the optimal transformation method in obtaining power series with well-behaved terms on the specific spin ($S = 1$) lattice of the hexagonal ferrimagnet $RbNiF_3$ is summarized and supplemented.

The organization of the paper is as follows: in Section 2 the high-temperature series expansion (HTSE) technique and the elaborated approach of optimal transformation of the expansion variable are shortly presented; in Section 3 the crystallographic and magnetic structure of $RbNiF_3$ are commented; Section 4 deals with experimental and theoretical results serving as a base for the three-dimensional spin model; Section 5 pays attention on some details of the HTSE analysis of the spin system and Section 6 summarizes main physical results.

2 The Method of High Temperature Series Expansion

In a zero magnetic field, the magnetic susceptibility is expanded in a power series in dependence of reciprocal temperature

$$\chi^{\mathrm{st}}(x) = \frac{S(S+1)x}{3}\Big(1 + \sum_{n=1}^{\infty} a_n(R,X)x^n\Big)\,, \tag{1}$$

where $x = |J_1|/kT$.

The function $\chi^{\mathrm{st}}(x)$ is continued analytically in the complex z-plane and the singularity of $\chi^{\mathrm{st}}(x)$ closest to the origin determines the radius of convergence of the power series [3, 4]. The methods of analysis significantly depend on whether this singularity corresponds to a critical point or not. When the closest point to the origin is the physical singularity, the different variants of the method of ratios [2] can be successfully applied. In the simplest variant of this method, the dependence of the ratios

$$\rho_n \equiv \frac{a_n}{a_{n-1}} = \frac{1}{x_c}\Big(1 + \frac{\gamma-1}{n}\Big) + O\Big(\frac{1}{n^2}\Big) \underset{n\to\infty}{\longrightarrow} x_c^{-1} \tag{2}$$

on the quantity $1/n$ is extrapolated to the limiting case $n \to \infty$ with the help of linear extrapolants:

$$\rho_n^{(1)} = n\rho_n - (n-1)\rho_{n-1}\,, \quad n = 2, \ldots, N\,. \tag{3}$$

From the asymptotic behavior of ρ_n, estimates can be obtained for the critical point x_c and the critical exponent γ.

In the case of oscillating series, an improvement of the estimates is achieved by taking into account the quantities

$$\tilde{\rho_n} \equiv \Big(\frac{a_n}{a_{n-1}}\Big)^{\frac{1}{2}} = \sqrt{\rho_n\rho_{n-1}}\,, \quad n = 2, \ldots, N\,. \tag{4}$$

In many cases it is necessary to conduct an even more detailed analysis of series coefficients with the help of the so-called Neville extrapolants:

$$\rho_n^{(r)} = \frac{1}{r}\left[n\rho_n^{(r-1)} - (n-r)\rho_{n-1}^{(r-1)}\right]\,, \quad 1 \le r \le n-1\,. \tag{5}$$

In the presence of disturbing singularities inside the physical disk $|z| \le x_c$, it is necessary to apply the technique of Padé approximations [14]. Padé approximants are a simple analytical continuation of the power series, which, in contrast to the

bare series, can represent simple poles in the complex plane and therefore may better approximate the original function.

By definition, the $[N, M]$ Padé approximant of the function $F(z)$ is the rational function

$$[N, M] \equiv \frac{P_N(z)}{Q_M(z)} = \frac{p_0 + p_1 z + \cdots + p_N z^N}{1 + q_1 z + \cdots + q_M z^N} \,, \tag{6}$$

where the coefficients p_i, q_i corresponding to the polynomial $P_N(z)$ of degree N and the polynomial $Q_M(z)$ of degree M, respectively, are chosen so that the expansion of $[N, M]$ agrees with the Taylor series expansion of $F(z)$, $z > 0$ to the order $N + M$.

Usually, the Padé approximants to the logarithmic derivative

$$\frac{d}{dx} \ln F(z) \equiv f(z) = \sum_n b_n z^n \tag{7}$$

are calculated. It is clear that if $F(z)$ is of the form

$$F(z) = (1 - yz)^{-\gamma} \Psi(z) \,, \tag{8}$$

where $\Psi(z)$ is an analytic function at point $z = y^{-1}$, then $f(z)$ has a simple pole at $z = y^{-1}$ and a residual γ. Therefore, estimates for y and γ can be obtained from the corresponding pole and residue of the Padé approximant.

The main idea of the Padé analysis of series with known first L-terms is to calculate the possible Padé approximants $[N, M]$ for all N and M such that $0 \leq N + M \leq L$. If the last significant digits in the results do not change substantially, the Padé table is considered to exhibit convergence. The question of the convergence of Padé's approximants (P.A.) is generally unclear and continues to attract the attention of mathematicians. In practice, it is believed sufficient to consider not the whole table, but a smaller triangular section symmetrical to the main diagonal of the table, i.e. P.A. $[N, M]$ [12]. Higher confidence is usually placed on balanced approximants, where the numerator and denominator are of approximately the same order. The structure of the poles of the approximant also requires in-depth attention.

It is often possible to achieve an improvement in the behavior of the series' coefficients, and hence the reliability of the estimates, by removing the strongly perturbing singularities outside the physical disk by prior transformation of the complex variable [9, 12].

In the case of only one pair of complex conjugate perturbing singularities, the optimal type of transformation is given by the expression

$$u = \frac{ABz}{\sqrt{(z - Be^{i\varphi})\,(z - Be^{-i\varphi})}} \,. \tag{9}$$

By appropriate selection of the parameters B, φ of the transformation, for each given pair of points, its moving to infinity can be achieved. It is often convenient to leave a point stationary through the replacement

$$A = \sqrt{1 - 2\frac{x_c^0}{B}\cos\varphi + \left(\frac{x_c^0}{B}\right)^2}. \tag{10}$$

The transformed function $g(u) \equiv \chi^{\mathrm{st}}(z(u)) = \sum\limits_{n=0}^{\infty} b_n(B\varphi)u^n$, where $z(u) = \dfrac{B_u}{\sqrt{A^2B^2 - u^2\sin^2\varphi} + u\cos\varphi}$ will exhibit the most regular behavior of the coefficients of the power series for the properly chosen B, φ. This behaviour however, will be perturbed by the singularities on the real axis introduced by the inverse transformation, of which the closest to the origin is a singularity at the point $u = AB$, for $\pi/2 < \varphi < \pi$ or at the point $u = -AB$ for $0 < \varphi < \pi/2$. We note that $AB > u_c > 0$, where u_c is the image of the critical point x_c. To partially compensate for this singularity, it was proposed [12, 15, 16] to conduct an optimized appropriate procedure for correcting the expansion of $g(u)$. In this procedure, it is conditioned that the choice of the transformation parameters should be based on the proposed optimization criterion – a minimum by the variables B and φ of the expression

$$Q(B,\varphi) = \sum_{n=1}^{N} w_n\left[\rho_n - \frac{1}{u_c}\left(1 + \frac{\gamma - 1}{n}\right)\right]^2, \tag{11}$$

where $w_n = n^2 / \sum\limits_{m=1}^{N} m^2$. It was shown that in this expression, instead of ρ_n, the quantities $\tilde{\rho_n}$ can also be used successfully.

To the optimally transformed series obtained, all standard methods of analysis are applicable. To obtain the coefficients of the optimally transformed series, a computer procedure was developed and used in the calculations [12, 16].

3 Crystal and Magnetic Structure of $RbNiF_3$

The hexagonal ferrimagnetic $RbNiF_3$ (Fig. 1) is isostructural with the hexagonal form of $BaTiO_3$. It features high transparency in the visible spectrum – the absorption factor is less than 1 cm^{-1} in the optical range 20 000–150 000 cm^{-1}. The geometric tolerance factor is on the border of the Goldschmidt criterion for the stability of the hexagonal over the cubic phase. In fact, this magnetodielectric is the 6H-type structural polytype synthesized at normal pressure. At elevated temperature and pressure, the hexagonal structure transforms to another phase, which is cubic perovskite, $a_0 = 4.074(2)$ Å [18]. The cubic phase was stable at ambient temperature

and was reported as antiferromagnetic with a Néel temperature of 260 K. The relative stabilities of these structural polytypes of $RbNiF_3$ versus applied pressure were investigated using the density functional theory (DFT) [19]. For the magnetic structure of cubic $RbNiF_3$, the simulations using the Vienna ab initio simulation package (VASP) yielded an antiferromagnetic G-type arrangement and an easy magnetization axis $\langle 111 \rangle$.

Detailed static and dynamic structural analysis has been reported on single crystals of hexagonal $RbNiF_3$ by X-ray diffraction [20] and inelastic neutron scattering [21], supplemented by conflicting neutron diffraction studies of the magnetic structure on single crystals [22] and powder samples [23, 24]. Complex spin models with different angles of inclination of the 2a and 4f sublattices to the c axis were considered [22] more acceptable than models of collinear ferrimagnetism. The controversy was solved by following the magnetic structure evolution with temperature by neutron powder diffraction (NPD) [25].

All structural reports confirmed that the compound adopts the hexagonal $D^4_{6h}(P6_3/mmc)$ space group symmetry with six formula units per unit cell. The Ni^{2+}

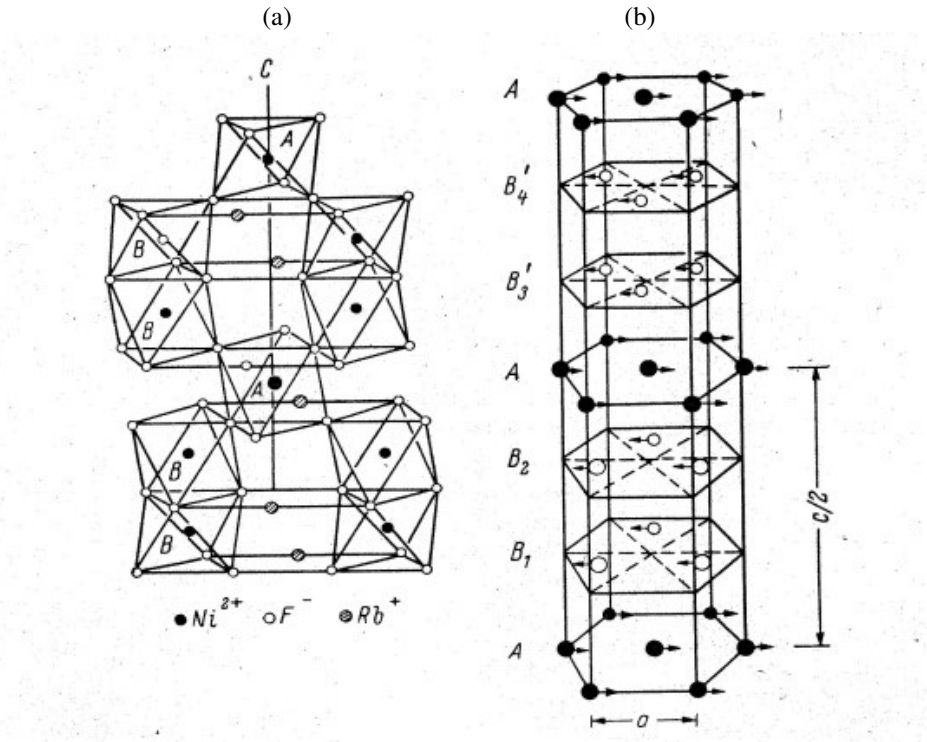

Fig. 1: Structure of hexagonal $RbNiF_3$: a) crystalline, b) collinear ferrimagnetic.

ions occupy two inequivalent 2a and 4f positions at the centre of a fluorine octahedron. Two-thirds of the NiF_6 octahedra occur in face-sharing pairs to form Ni_2F_9 polyhedra. The remaining NiF_6 octahedra are linked to the Ni_2F_9 polyhedra by sharing of vertices, Fig. 1a). Of interest is the fact that the average length of the Ni^{2+}–F^- bond equal to 2.028 Å [20, 25], is almost exactly in accordance with the empirical ionic radii of these two ions in perovskite-like fluorides, which is an indication of the ionic nature of the compound. Ni (B) ions form pairs at a distance of 2.728 Å, and the angle of superexchange interaction is 84.1°, i.e. approximately 90°. The distance Ni (A) – Ni (B) is significantly greater, equal to 4.034 Å, the bond angle Ni(A) – F^- – Ni(B) is 178.2°, i.e. near 180°.

Different values ranging from 133 to 145 K have been reported for the magnetic order transition temperature [21–29]. Here is to note that $T_N = (135 \pm 0.5)$ K was determined from the temperature dependence of reflection (002) and the maxima of (100) and (103) reflections with a significant magnetic contribution to the neutron diffractograms [25]. From magnetic [27, 28], magneto-optical [26, 28, 29], elastic and inelastic neutron scattering [21] and NPD [23–25] experiments, it was concluded that at liquid helium temperatures the Ni^{2+} magnetic moments lie in the basal plane forming two inequivalent magnetic sublattices, Fig. 1b. The anisotropy field is small in the basal plane (-0.2 kOe) but sufficient to cant the spins from the plane to the optical axis (16–20 kOe) [26].

4 Description of the Spin System

The Ni^{2+} ions, lying in equivalent layers with stacking sequence ABBAB′B′A ..., carry an equal spin ($s = 1$). They are coupled by superexchange by way of the intervening F ions, Fig. 2a). The dominant interactions by way of one F ion, are the close to 180° antiferromagnetic exchange between nearest-neighbour A,B and A,B′ Ni ions, and the close to 90° ferromagnetic exchange between nearest-neighbour (in adjacent layers) B,B and B′,B′ ions. They determine the antiparallel spontaneous alignment of the spins in the A and B layers below T, and so the ferrimagnetism of $RbNiF_3$. In a good approximation, this compound has magnetic anisotropy of an "easy-plane"-type.

Summarizing the ordering scheme, the magnetic ions occupy the sites on equivalent plane triangular lattices A,B,B′ mutually translated, as depicted in Figure 2, b), and are ordered in the sequence ABBAB′B′ABB ... The distance between neighbouring A and B planes is equal to the distance between neighbouring A and B′ planes and similarly the distances between neighbouring B,B and neighbouring B′,B′ planes are equal. According to [21, 27, 29], the magnetic structure of $RbNiF_3$, is determined essentially by interplanar interactions: between nearest-neighbour A, B and A, B′ spins and between nearest-neighbour B, B and B′, B′ spins. For these two basic ex-

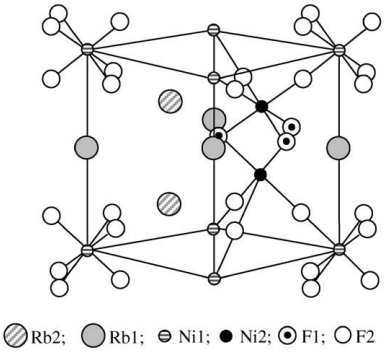

(a)

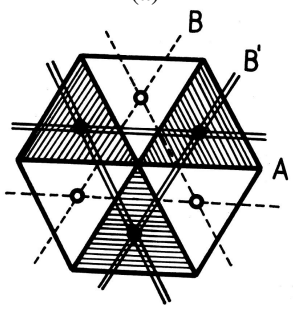

(b)

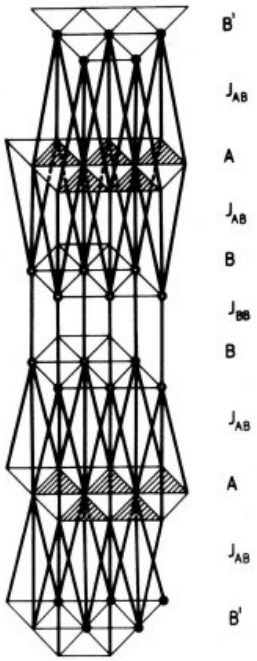

(c)

Fig. 2: a) One half of the hexagonal unit cell of $RbNiF_3$; b) The Ni^{2+} ions occupy the sites of symmetrical1y translated equivalent plane triangular lattices A, B, B′; c) The dominant interactions are depicted by inclined and vertical solid lines.

change parameters, the analyses of the spin-wave scattering neutron data [21] gave the estimate of -93.2(2) K for the antiferromagnetic exchange and 21.1(2) K for the nearest neighbour ferromagnetic exchange.

Thus, the spin system may be described by the Heisenberg model with two different (opposite signs) first-neighbour exchange constants: $J_{\mathrm{AB}}(= J_{\mathrm{AB}'}) < 0$ and $J_{\mathrm{BB}}(= J_{\mathrm{B}'\mathrm{B}'}) > 0$. In Fig. 2c) these interactions are depicted with inclined and vertical lines, respectively.

The Hamiltonian of such a system of N spins in an external magnetic field h (in the direction of the z axis) is

$$H = -J_{\mathrm{AB}} \sum_{\langle ab \rangle} \boldsymbol{S}_a \cdot \boldsymbol{S}_b - J_{\mathrm{BB}} \sum_{\langle bb \rangle} \boldsymbol{S}_b \cdot \boldsymbol{S}_b - \mu_{\mathrm{B}} g h \left(\sum_b S_b^z - \sum_a S_a^z \right), \tag{12}$$

where S_i $(i = x, y, z)$ are the spin operators in the site a; the first two sums are

over nearest neighbour A,B and A,B′ spins and over nearest neighbour B,B and B′,B′ spins respectively, g is the gyromagnetic ratio and μ_{B} is the Bohr magneton.

We denote: $R = J_{\mathrm{BB}}/J_{\mathrm{AB}}$, $x = |J_{\mathrm{AB}}|/kT$, $X = s(s+1)$

$$P = \sum_{\langle ab\rangle} \boldsymbol{S}_a \cdot \boldsymbol{S}_b + R \sum_{\langle bb\rangle} \boldsymbol{S}_b \cdot \boldsymbol{S}_b \,,$$
$$Q = \sum_b S_b^z + \sum_a S_a^z \,, \quad Q' = \sum_b S_b^z - \sum_a S_a^z \,. \tag{13}$$

The high-temperature series expansion of the physical susceptibility per spin in a zero external field is

$$\chi^{\mathrm{ph}}(0)/N = \left(g^2\mu_{\mathrm{B}}^2 X/3kT\right)\left(1 + \sum_{n=1}^{\infty} x^n a_n\right). \tag{14}$$

The coefficients a are given by the expression

$$a_n = \frac{2(\operatorname{sgn} J_{\mathrm{AB}})^n}{(n+2)!}\frac{3}{X}\left(\text{coeff. of } N \text{ in } \frac{\mathrm{Tr}\left\{P^n Q^2\right\}}{(2s+1)^N}\right), \tag{15}$$

where $\{P^n Q^2\}$ denotes a sum over all permutations of nP factors and two Q factors.

The staggered susceptibility for the ferrimagnetic ordering of the spins ($J_{\mathrm{AB}} < 0$; $J_{\mathrm{BB}} > 0$) is expanded

$$\chi^{\mathrm{st}}(0)/N = (g^2\mu_{\mathrm{B}}^2 X/3kT)\left(1 + \sum_{n=1}^{\infty} x^n a_n{}'\right). \tag{16}$$

The coefficients $a_n{}'$ differ from the corresponding a_n by the replacement of Q with Q'.

The technique of explicit computation of the coefficients is discussed in detail in [13, 15, 16].

The internal energy of the spin system is $\mathcal{E} = kT^2\dfrac{\partial(\ln Z)}{\partial T}$, where the partition function $Z = \mathrm{Tr}e^{-\frac{H}{kT}} = (2s+1)^N[1 + \sum\limits_{n\geq 1}\dfrac{(\operatorname{sgn} J_{\mathrm{AB}})^n}{n!}x^n\dfrac{\mathrm{Tr}\{P^n\}}{(2s+1)^N}]$, the trace Tr is taken over the $(2s+1)^N$-dimensional space, and N is the number of spin lattice sites. In zero magnetic field, for the specific heat $C(0)$ per spin in dimensionless units we have [17]

$$\frac{C(0)}{Nk} = \frac{1}{Nk}\frac{\partial \mathcal{E}}{\partial T} = x^2\frac{\lambda_2}{N}(1 + \sum_{n\geq 1} x^n \frac{(\operatorname{sgn} J_{AB})^n}{n!}\frac{\lambda_{n+2}}{\lambda_2}$$
$$= x^2\frac{\lambda_2}{N}\Big(1 + \sum_{n\geq 1} x^n c_n\Big)\,, \tag{17}$$

where $\lambda_m = N\Big[\dfrac{\operatorname{Tr} P^m}{(2s+1)^N}\Big]\,, \quad m = 2, 3, \ldots$

As we have already noted, the coefficients c_n are directly related to the high-temperature behavior of such thermodynamic quantities as internal energy $\mathcal{E}$, entropy S, the logarithm of the partition function $\ln Z$, etc.

Integrating the equalities $\dfrac{\partial \mathcal{E}}{\partial T} = C(0)$, $\dfrac{\partial S}{\partial T} = \dfrac{1}{kT}C(0)$, we obtain

$$\frac{\mathcal{E}(\propto) - \mathcal{E}(T)}{NkT} = \frac{\lambda_2}{N}x^2 \sum_{n\geq 0}\frac{c_n}{n+1}x^n\,, \tag{18}$$

$$\frac{S(\propto) - S(T)}{N} = \frac{\lambda_2}{N}x^2 \sum_{n\geq 0}\frac{c_n}{n+2}x^n\,. \tag{19}$$

For the partition function holds

$$\frac{1}{N}\ln Z = \ln(2s+1) + \frac{\lambda_2}{N}x^2 \sum_{n\geq 0}\frac{c_n}{n+1}x^n\,. \tag{20}$$

In (18), (19) and (20) $c_0 = 1$ and bearing in mind the relations $\mathcal{E} = -J_{AB}\dfrac{\partial(\ln Z)}{\partial x}$, $S = \ln Z - x\dfrac{\partial(\ln Z)}{\partial x}$, from (20) one may conclude that the high-temperature limits $\mathcal{E}(\propto) = 0$ and respectively $S(\propto) = N\ln(2s+1)$.

The expressions for the coefficients a_n in (15), $a_n{}'$ in (16), and c_n in (17) – (20) were calculated in terms of the graph theory [3] elaborated to apply the HTSE technique to the Heisenberg model [2, 4], but adapted to suit the studied spin system. Here is to recall that a localized graph of the n-th order ($n \geq 1$) is named any set of n lines with a fixed position on the interaction scheme illustrated in Fig. 2, i.e. connecting in a certain way (possibly by multiple lines) the vertices in the scheme. Details of the adapted graph technique [3] concerning the graph configurations G, mean reduced traces (MRT) of configurations <G>, occurrence factors Ng and weights of the configurations Wg, are presented in [13, 15, 17].

In Appendix A: we tabulate $a_n = a_n(R, X)$ and $a_n{}' = a_n'(R, X)$ up to $n = 6$, whereas the coefficients of specific heat c_n up to $n = 5$ are given in Appendix B:.

5 Analysis of the High-Temperature Series of the Compound $RbNiF_3$

The analysis of the truncated power series of the physical susceptibility did not give a clear indication of the presence of a critical point because of the short number of terms of the series. Therefore, we examined in more detail the series expansion of the staggered susceptibility. Preliminary estimates of the critical point and the distribution of other singularities that perturb the behavior of series coefficients were obtained by the ratio method and from the Pad approximants to the logarithmic derivative of the initial series.

The analysis of the initial series for the staggered susceptibility in the spin system model studied, which were constructed for spin $S = 1$ and an exchange constants ratio R in the interval $-3.0 \leq R \leq -0.2$ shows that the main perturbing singularities lie inside the physical disk $|z| \leq x_c$. This resulted in a pronounced irregular behaviour and significant oscillations of the series coefficients. The oscillations decreased only in a narrower range $-0.8 \leq R \geq -1.0$ and the presence of a critical point became clear for R around the value $R = -1$.

To extract reliable information made it necessary to eliminate the perturbing irregularities by an appropriate procedure. To more clearly determine the position of the main perturbing singularities inside or near the physical disk, we constructed the Padé approximants to the series

$$(z-p)(z-p)^* \frac{d}{dx} \ln \chi^{\mathrm{st}} \quad \text{or} \quad (z-q) \frac{d}{dx} \ln \chi^{\mathrm{st}}\,, \tag{21}$$

where the perturbing complex conjugate pair of poles (or real pole) is removed directly. For some of the series, it proved to be effective a prior transformation of the expansion variable by a transformation of Euler-type

$$u = \frac{Az}{1 + z/B} \quad \text{or} \quad = \frac{Az}{1 + zB^{-1}}\,. \tag{22}$$

The parameters A and B were chosen so that the physical singularity does not change and remains a fixed point, while the main interfering singularity, expressed in the new variable, to be moved as far as possible distant from the origin [14], i.e. to attain the maximum modulus of the pole image at a fixed u_c. When the spurious pole u^{sp} introduced by the transformation was close to the physical pole, its influence was reduced by considering the function $(1 - u/u^{\mathrm{sp}})\chi^{\mathrm{st}}(x(u))$ instead of $\chi^{\mathrm{st}}(x(u))$ [30]. At the same time, with the aim of producing the best result, the effective exponent γ was taken as a variable. The criterion for the best result was the consistency of the estimates obtained by the method of ratios with those through the Padé analysis. For this purpose, we have compiled a computer program to implement the algorithm described above.

The dependences of the ratios of the coefficients of the transformed and corrected series of staggered susceptibility as well the singularities revealed through the Padé analysis in their Padé approximants are displayed and commented in [15]. The presented results were obtained for $R = -0.226$, -1.0, and -2.354, respectively and clearly demonstrated the very positive effect of applying the method of optimal transformation.

The transformation of the Euler type, which is a special case (for $\varphi = \pi$) of the transformation (9), proved to be effective only for a small part of the series. Nevertheless, we were able to obtain the critical point estimates using the features of the Padé approximants [3,2], [2,3], [1,4] and [2,2] (in the Padé analysis) and the Neville extrapolants $\rho_n^{(1)}$, $\rho_n^{(2)}$ for $n = 5.6$ (the ratios method).

In the later stage of our work, the transformation of the series we performed by applying the method of the optimal transformation implementing two criteria for optimality. In the first variant, in the quadratic form (11) we used the ratio of the coefficients determined by the formula (2), and in the second – the values for the $\tilde{\rho_n}$ determined by (4). The minimum of the form (11) was sought in the angular range $90^\circ < \varphi < 180^\circ$.

Table 1 shows the estimates for the critical parameters obtained at the R values given in the first column. The first three columns for each of the criteria display the used values of x_c and the optimal parameters B and φ, which were obtained by applying the procedure for self-consistent correction of the transformed series. In the fifth and tenth columns, respectively, estimates are given for the critical point x_c and the critical exponent γ (in parentheses), which are obtained using the corresponding criterion of optimality, as well as their scatter range. The values of x_c and γ slightly change when calculated by averaging Neville extrapolants $\rho_5^{(1)}$, $\rho_6^{(1)}$, $\rho_5^{(2)}\rho_6^{(2)}$ and are even closer to the Padé estimates. In the sixth and eleventh columns are given for each criterion, respectively, the estimates assigned by averaging the PA [2,2], [3,2], [2,3] and [1,4] for the logarithmic derivative of the optimally transformed series.

In general, after applying the method of optimal transformation with partial correction for the imported singularities, a satisfactory agreement is reached between the estimates by the method of the ratios with those obtained by the method of Padé approximants. The agreement does not depend on which quantity, either ρ_n or $\tilde{\rho_n}$, is used in the criterion for optimality of the transformation. The difference in the estimates of the critical point by the two criteria generally does not exceed the magnitude of the uncertainty of the respective values.

As mentioned, the above results were obtained by direct analysis of the coefficients of the transformed series, without applying modified methods for extracting information from the series analysis [3, 14]. Based on the results in [12], such a re-

Table 1: Results obtained by the method of optimal transformation (for designations see the text)

-R	Criterion ρ					Criterion $\tilde{\rho}$				
	Optimal parameters			Ratio	Padé	Optimal parameters			Ratio	Padé
	x_c^0	B	φ^0	method	analysis	x_c^0	B	φ^0	analysis	analysis
0.2	0.74	0.826	180	0.706_9 (1.93_4)	0.709_8	0.74	0.452	180	0.799_2 (1.964_1)	0.719_{11}
0.226	0.70	0.813	180	0.695_8 (1.90_3)	0.699_5	0.70	0.446	180	0.6998_5 (1.940_1)	0.704_9
0.4	0.68	0.746	180	0.637_1 (1.758_5)	0.635_8	0.68	0.446	180	0.6407_1 (1.788_1)	0.6391_8
0.6	0.60	0.649	151	0.5876_6 (1.622_3)	0.590_4	0.60	0.429	148	0.5925_1 (1.663_1)	0.590_4
0.8	0.58	0.610	140	0.553_1 (1.532_6)	0.557_1	0.58	0.415	130	0.5547_5 (1.553_1)	0.557_1
1.0	0.564	0.613	123	0.5243_9 (1.446_6)	0.5257_3	0.50	0.454	100	0.5267_2 (1.479_1)	0.521_4
1.2	0.54	0.617	125	0.507_2 (1.421_7)	0.507_3	0.60	0.606	92	0.508_2 (1.45_1)	0.501_4
1.4	0.52	0.502	167	0.501_4 (1.464_7)	0.490_8	0.50	0.8626	180	0.5096_8 (1.527_3)	0.496_1
1.6	0.50	0.448	180	0.489_3 (1.442_2)	0.492_5	0.50	0.294	180	0.4965_7 (1.496_2)	0.489_3
1.8	0.50	0.400	180	0.478_3 (1.416_8)	0.484_2	0.50	0.269	180	0.4860_8 (1.470_3)	0.472_{12}
2.0	0.48	0.372	162	0.467_3 (1.38_1)	0.466_6	0.48	0.247	180	0.477_1 (1.450_4)	0.465_9
2.2	0.46	0.658	117	0.450_2 (1.297_8)	0.448_1	0.46	0.227	106	0.4565_5 (1.384_3)	0.450_9
2.354	0.45	0.535	124	0.444_2 (1.27_2)	0.442_1	0.45	0.709	114	0.4489_3 (1.340_1)	0.438_4
2.6	0.44	0.435	128	0.433_3 (1.22_2)	0.4312_1	0.44	0.463	120	0.4367_4 (1.274_1)	0.428_3
2.8	0.44	0.395	128	0.424_4 (1.19_2)	0.4226_8	0.44	0.412	122	0.4270_1 (1.222_1)	0.420_2
3.0	0.44	0.361	128	0.416_4 (1.15_3)	0.4145_6	0.44	0.374	123	0.4175_1 (1.171_1)	0.4117_2

finement of estimates is unlikely to affect our values with a change exceeding 1-3%. It should be noted that the P.A. to the logarithmic derivative, for example at $R = -1.0$, gave a clear indication of the presence of a pair of complex conjugate singularity z_1, z_1^* with modulus $|z_1| \cong 0.7 - 0.8$ and argument $\varphi \cong 117^\circ - 129^\circ$, which are very close to the points $z = Be^{\pm i\varphi}$, removed by the optimal transformation ($B = 0.61$, $\varphi = 123^\circ$), in the case of using the ratios ρ_n. The situation is similar for the series at $R = -1.2$.

For the specific high-temperature series of the staggered susceptibility of $RbNiF_3$, the introduction of the quantity $\tilde{\rho_n}$ in the criterion for optimality of the transformation leads to a small systematic increase of the estimates by the method of ratios for both critical points and critical exponents compared to those obtained using ρ_n ratios. It can be shown that for most of the series the analysis of P.A. shows the presence of complex conjugate basic perturbing singularities inside the physical disk, while the quantity $\tilde{\rho_n}$ is effective for smoothing oscillations in the behavior of the series caused by the presence of a perturbing singularity located on the real axis.

The estimates of the critical exponent γ change smoothly in the interval $1.15 \leq \gamma \leq 1.96$ with varying R in the interval $-3.0 \leq R \leq -0.2$. Given the known difficulties in obtaining an accurate estimate of the critical exponent γ [30] even at satisfactory accuracy of the estimate of x_c [14] as well as the fact that the model of a spin system with two exchange interactions we are considering is emphatically open, and that in such cases the actual asymptotic behaviour of the series is reached at a higher number of expansion coefficients, especially at very high and very low values of R, we consider that the estimates of γ presented by us can be considered most probably illustrative, and certainly not as an indication of a violation of the hypothesis of universality. Nevertheless, it is worth noting that for R between -1.0 and -2.0, where the original and transformed series of staggered susceptibility behave best, γ^{st} is close to 1.4 within 3%, which is in reasonable agreement with the current value of $\gamma = 1.3960(9)$ for the three-dimensional Heisenberg universality class.

In the work of Paul and Stanley [30], an Ising model with spatial anisotropy (different constants of interaction in different directions in the lattice) is considered. As shown there, for some values of the ratio R, estimates for γ can be obtained on the basis of the corresponding truncated series, which are not in agreement with the hypothesis of universality. In such cases, these authors express the opinion that the series are not long enough to obtain a correct estimate of γ. In addition, Hunter and Baker [14], based on the study of a number of test functions, show cases of unsatisfactory estimation of γ even in the case of rather long series, while the critical point x_c is quite accurately estimated by power series with a smaller number of coefficients.

In the whole range of values of the ratio of the exchange constants R in the studied case, the obtained estimates for γ are closer to the expected value 1.4 than in the

case of using traditional methods of analysis of the same series without prior transformation of the variable by the optimal method [12, 15]. Taking into account the results in [12, 13], we believe that the method of optimal transformation gives more reliable estimates for the critical temperature, especially for values of R: $R \leq 0.4$ and $R \geq 0.4$, compared to those [13] previously obtained.

6 Remarks on the Comparison with Results for $RbNiF_3$

Figure 3 gives the estimates of the possible pairs of exchange constants in the interval $-3.0 \leq R \leq -0.2$ corresponding to the critical points x_c after implementing the optimal transformation method. Curve 1 represents the possible pairs calculated using the critical point $x_c = T_{\text{exp}} = 133$ K [21] for the transition from ferrimagnetic to paramagnetic state. Curve 2 was calculated for $x_c = T_{\text{exp}} = 156$ K, which is based on the estimates $J_{\text{AB}} = -69.1$ K, $J_{\text{BB}} = 162.7$ K given in [29].

It should be noted that previous theoretical estimates of the magnetic transition temperature extracted by various modifications to the effective field theory differ significantly, by more than 20%, from the experimental value. The closest estimate is $T_c^{\text{th}} = 163$ K [29] when considering a quantum mechanical model of the spin system in a cluster approximation of the Bethe-Peierls-Weiss (BPW) type, taking into account the interactions between the nearest neighbours. In the same work, the very reasonable estimate $T_c^{\text{th}} = 135$ K was obtained also within the classical BPW method, but taking into account the additional inclusion of exchange interactions between more distant neighbours in the cluster spin model. This closer agreement with the experimental transition temperature was reached after a large number of assumptions and approximations in the treatment of the spin model. Therefore, it can be

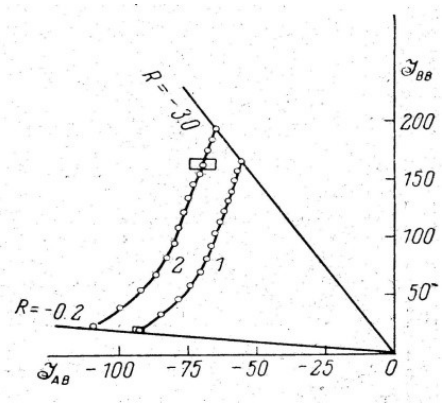

Fig. 3: Possible exchange constants.

considered as a purposeful deliberate assessment, reflecting and relying exclusively on the physical intuition of the authors.

As already mentioned in the introductory part, the representation of a given thermodynamic function by a high-temperature series expansion can be compared with its experimentally determined temperature dependence. The magnetic susceptibility of the compound $RbNiF_3$ above the critical point, i.e. in the paramagnetic region, was measured and discussed first by Smolensky et al. [27] followed by Schafer et al. [28] in more details. Figure 4 shows the calculated behaviour of the physical magnetic susceptibility, based on the first six coefficients in the high-temperature series expansion that are displayed in the Appendix. The curves presented were calculated for the two values of the gyromagnetic ratio of Ni ion, which are cited most often in the literature: $g = 2.35$ (crosses) and $g = 2.29$ (points). The very good agreement of the experimental curve [28] with one of the calculated curves, namely that for $g = 2.29$, can serve as an indication of the correct value of the Landé factor in this case, as this is the only parameter determining the slope of the high-temperature asymptote to reciprocal magnetic susceptibility.

As can be seen from Fig. 4, from the initial six coefficients of the high-temperature

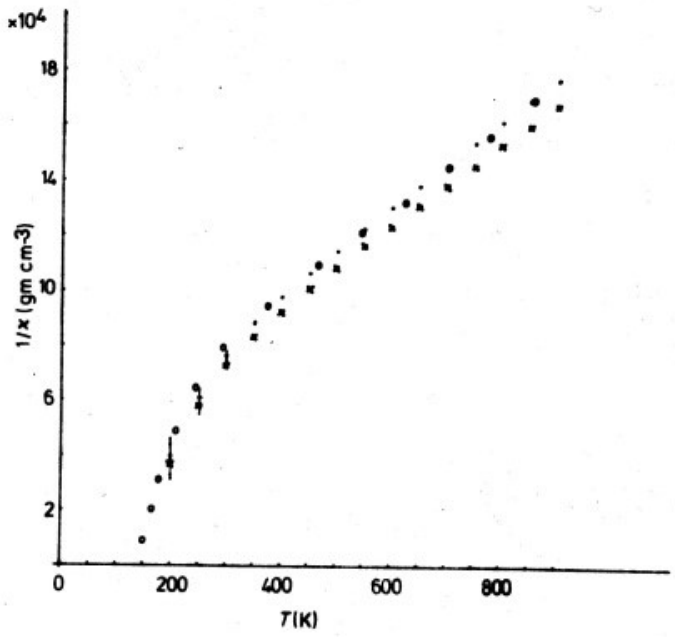

Fig. 4: Inverse susceptibility versus temperature.

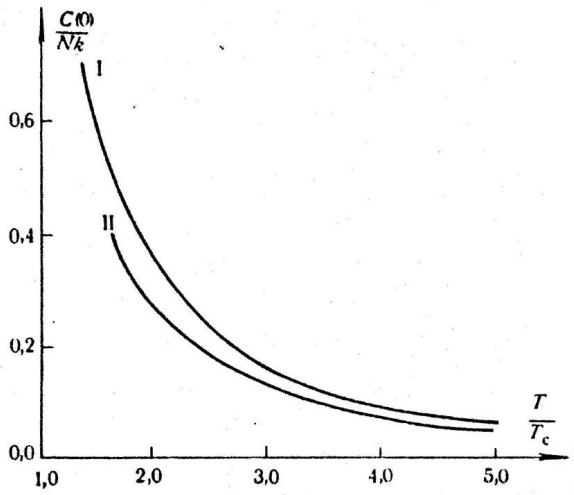

Fig. 5: Specific heat per spin versus relative temperature T/T_c ($T_c = 133$ K).

series, the behavior of magnetic susceptibility close to the critical point T_c could not be reliably described. At a temperature of 200 K, the inaccuracy caused by the truncation of the series has been estimated about 15%. At higher temperatures, it decreased rapidly and at 300 K the uncertainty became below 1%. The assessment of uncertainty was based on the contribution of the last available partial sum of the series.

The analyses of the heat capacity series corresponding to $RbNiF_3$ based on the available Pad approximants did not reveal a critical point. Figure 5 shows the calculated heat capacity curves for the two sets of the exchange constants given in [21] and [29], respectively. It is interesting to note that the first set of exchange constants [21] represents the behavior of $C(0)/Nk$ from a temperature closer to T_c ($T/T_c = 1.3$) compared to that ($T/T_c = 1.7$) for the second set of constants [29].

The very good agreement of the experimental temperature of the magnetic transition with the estimate of x_c obtained by the HTSE method for the Heisenberg model with two exchange constants of opposite sign, whose numerical values are estimated in [21], should not be considered to happen accidentally, given the reliability of the HTSE method for three-dimensional quantum mechanical models. This compliance undoubtedly reflects the physical content of the quantum model of the studied spin system and may be regarded as a confirmation of the correctness of the considerations indicated in [19,21] and to great extent in [31] for the determining spin interactions in the hexagonal $RbNiF_3$. First-principles calculations, based on density functional theory (DFT) using the generalized gradient approximation exchange-correlation func-

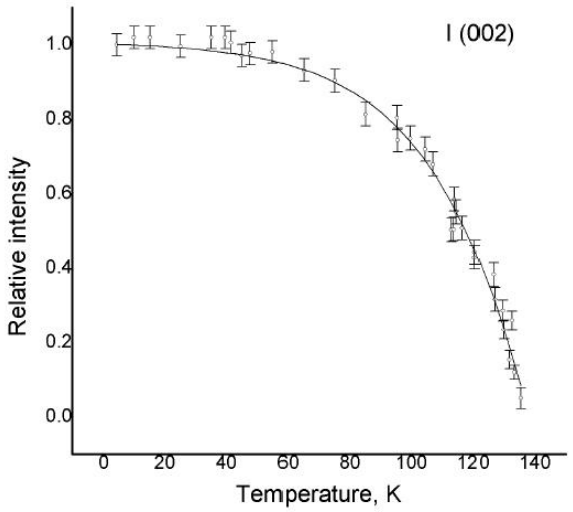

Fig. 6: Temperature dependence of the integrated intensity of reflection (002).

tional with included Hubbard correction term, (GGA+U) approach, have indicated that the hexagonal $RbNiF_3$ is a direct zone semiconductor. It is a Mott type insulator, where the bandgap of 5.12 eV is determined by the splitting of Ni $3d$-levels [19].

The understanding that the studied system is indeed a three-dimensional collinear Heisenberg ferrimagnet finds evidence in all available experimental data. The 3-D character of the phase transition is consistent with both the inelastic neutron scattering findings [21] and the magnetic structure evolution [25]. Figure 6 presents the result of the neutron diffraction measurement of the temperature dependence of the integrated intensity of reflection (002), which is almost entirely of magnetic origin [25]. The measured intensities were corrected for the nuclear scattering contribution. Then, the square roots of data correspond to the spontaneous magnetization M_s and in the temperature region $0.88 < T/T_N < 0.98$ they were fitted to the power-law $B(1 - T/T_N)^{\beta}$ by a least-squares analysis, in which each data point was weighted inversely proportional to its estimated uncertainty. For the critical exponent β of the thermal behaviour of magnetization close to the magnetic phase transition, the analysis yielded $\beta = 0.34 \pm 0.03$. The inclusion of data corresponding to temperatures below 119 K deteriorated the fit quality indicating the breakdown of the power-law behaviour away from T_N. It is noteworthy that the theoretical prediction for this critical exponent of the three-dimensional Heisenberg model is $\beta' = 0.365$. Thus, the value of the exponent found for $RbNiF_3$ is consistent with the exponent expected for isotropic magnets belonging to the Heisenberg universality class with short-range exchange in three dimensions, although the value estimated by us experimentally is

somewhat low. The analyses indicated that as the temperature increases, $T \to T_N$, the sublattice magnetizations smoothly decrease. The two sublattice collinear ferrimagnetic structure of ferroxplan type that is effective at the temperature of liquid helium and above up to about 50 K transforms into a canted structure with spins gradually out of the basal plane. The particular spin arrangement can be viewed as a set of 'two-dimensional ferrimagnets' composed of three successive planes f–a–f, coupled internally by strong exchange field $H_{\rm af}$, which are then aligned to each other by the much smaller exchange field $H_{\rm ff}$: The phase transition may be regarded as a disordering of these three-plane 'twodimensional ferrimagnets' relative to each other but with the planar units remaining well correlated.

7 SUMMARY

We have applied the high-temperature expansion method to investigate the J_1–J_2 Heisenberg model's thermodynamic quantities on a hexagonal lattice. The power series were analysed with the method of optimal transformation. AFM and FM nearest-neighbour exchange interactions J_1 and J_2, respectively, were considered. Numerical results for magnetic susceptibility and specific heat as a function of temperature are presented for different ratios of exchange couplings $R = J_2/J_1$ in a wide interval $-3.0 \leq R \leq -0.2$ ($J_1 < 0$, $J_2 > 0$) and arbitrary spin S. Based on the series expansions, the behaviour of the magnetic susceptibility and specific heat by taking into account the dominant coupling constants and the spin number $S = 1$ valid for ferrimagnetic $RbNiF_3$ is presented and compared with available theoretical and experimental data. The scheme of spin-spin interactions is open, in the sense that the neighbours to whom a given site is coupled do not interact with each other. Expectedly, the series of specific heat are not sufficiently long to reveal a critical point. Nevertheless, it is demonstrated that the presented expansions can be used to get useful information on the ratio J_2/J_1, e.g., from susceptibility measurements. Although the number of coefficients in these expansions may be regarded as comparatively few, the series of staggered susceptibility show reasonable convergence and the critical points x_c have been determined with convincing precision. Also shown is that literature data for the temperature dependence of inverse susceptibility provide strong evidence on the spectroscopic Landé factor of Ni^{2+} ion in $RbNiF_3$.

ACKNOWLEDGMENTS

This work was supported by the Bulgarian National Science Fund under Grant КП-06-India-2/2018 (Bulgaria-India Joint Research Projects scheme).

APPENDIX A:

We write the expressions for the coefficients $a_n(RX)$ and $a_n{}'(RX)$ in tabular form, the numerical coefficient within the table multiplying both the power of X above and

the power of R in the left.

$a_1 = \text{sgn}\, J_{\text{AB}} \frac{2}{9} X(6+R)$

$a_2 = \frac{1}{18} X$

	1	X
1	-6	+28
R		+8
R^2	-1	

$a_3 = \text{sgn}\, J_{\text{AB}} \frac{1}{135} X$

	1	X	X^2
1	+12	-117	+188
R		-15	+130
R^2		-15	
R^3	+2	-2	-2

$a_4 = \frac{1}{3240} X$

	1	X	X^2	X^3
1	-90	+1482	-4392	+4608
R		+96	-1416	+3904
R^2		+180	-740	+400
R^3		+96	-96	-96
R^4	-15	+30	+20	

$a_5 = \text{sgn}\, J_{\text{AB}} \frac{1}{340200} X$

	1	X	X^2	X^3	X^4
1	+3456	-75546	+365454	-595440	+374720
R		-3150	+70455	-362880	+603120
R^2		-6300	+59850	-93800	+84000
R^3		-6300	+27090	-38640	-21840
R^4		-3150	+6300	+4200	
R^5	+576	-1566	-201	+720	+480

$a_6 = \frac{1}{4082400} X$

	1	X	X^2	X^3	X^4	X^5
1	-17388	+456120	-3146808	+7468272	-8284416	+4258240
R		+13824	-385344	+2867976	-7636800	+7479680
R^2		+29862	-502047	+1534848	-2228240	+2587200
R^3		+26964	-248220	+562968	-612640	-327936
R^4		+29862	-140112	+233268	+38640	-67200
R^5		+13824	-37584	+4824	-17280	+11520
R^6	-2898	+9324	-3423	-6216	-3360	

$a'_1 = \frac{2}{9} X(6-R)$

$a'_2 = \frac{1}{18} X$

	1	X
1	-2	+28
R		+8
R^2	-1	

$$a'_3 = -\frac{1}{135}X$$

	1	X	X^2
1	+3	+47	-188
R		-5	+130
R^2		+15	
R^3	+2	-2	-2

$$a'_4 = \frac{1}{3240}X$$

	1	X	X^2	X^3
1	-18	+6	-2136	+4608
R		+24	+376	-3904
R^2		+96	-740	+400
R^3		-96	+96	+96
R^4	-15	+30	+20	

$$a'_5 = -\frac{1}{340200}X$$

	1	X	X^2	X^3	X^4
1	-576	-4086	-34746	+272880	-374720
R		-630	+1995	-157920	+603120
R^2		-2100	-26670	+79800	-84000
R^3		-3780	+24570	-40320	-21840
R^4		+3150	-6300	-4200	
R^5	+576	-1566	-201	+720	+480

$$a'_6 = \frac{1}{4082400}X$$

	1	X	X^2	X^3	X^4	X^5
1	-2484	+35856	+22848	+1335232	-4537216	+4258240
R		+2304	-26424	+40776	+2811840	-7479680
R^2		+8442	-54627	+877408	-1724240	+2587200
R^3		+10044	+96492	-365736	+700000	+327936
R^4		+19602	-119232	+241668	+38640	-67200
R^5		-13824	+37584	+4824	-17280	-11520
R^6	-2898	+9324	-3423	-6216	-3360	

APPENDIX B:

Coefficients of high-temperature expansion of specific heat for arbitrary values of exchange constants and spin s ($X = s(s+1)$).

$$\frac{\lambda_2}{N} = \left(\frac{a^2}{3} + 2\right)\frac{X^2}{3}$$

$$c_1 = -\frac{(\mathrm{sgn}\, J_{\mathrm{AB}})}{8(a^2+6)}(a^3+6)$$

$$c_2 = -\frac{1}{20(a^2+6)}$$

	1	X	X^2
1	6	-41	14
a^2		-10	
a^4	1	-1	-1

$$c_3 = -\frac{(\mathrm{sgn}\, J_{\mathrm{AB}})}{144(a^2+6)}$$

	1	X	X^2
1	-18	246	-56
a^2		30	
a^3		30	
a^4	-3	6	4

$$c_4 = \frac{1}{60480(a^2+6)}$$

	1	X	X^2	X^3	X^4
1	3456	-66726	176664	-84720	7360
a^2		-5670	52920	-11760	16800
a^3		-5040	1260		
a^4		-5670	7560	5040	
a^6	576	-1566	-201	720	480

$$c_5 = -\frac{(\mathrm{sgn}\, J_{\mathrm{AB}})}{86400(a^2+6)}$$

	1	X	X^2	X^3	X^4
1	-2484	59148	-292860	142456	-7360
a^2		4032	-61152	14168	-11200
a^3		3276	-30366	8064	-56000
a^4		3276	-5166	-2016	
a^5		4032	-9072	-3192	
a^7	-414	1332	-489	-888	-480

REFERENCES

[1] M.F. FISHER (1968) The theory of equilibrium critical phenomena. *Reports on Progress in Physics* **31**(1) 418-420 (corrigenda and addenda to *Reports on Progress in Physics* (1967) **30** 615-7300; DOI: https://iopscience.iop.org/article/10.1088/0034-4885/31/1/508/pdf.

[2] G.S. RUSHBROOKE, G.A. BAKER, P.J. WOOD (1974) Heisenberg Model, Chapter 5. In: C. Domb, M.S. Green (eds), "Phase Transitions and Critical Phenomena", volume 3 "Series expansions for lattice models". New York: Academic Press.

[3] C. DOMB (1970) Series expansions for ferromagnetic models. *Advances in Physics* **19** 339-370; DOI: https://doi.org/10.1080/00018737000101131.

[4] C. DOMB (1974) Graph Theory and Embeddings, Chapter 1. In: C. Domb, M.S. Green (eds) "Phase Transitions and Critical Phenomena", volume 3 "Series expansions for lattice models". New York: Academic Press.

[5] A. HEHN, N. VAN WELL, M. TROYER (2017) High-temperature series expansion for spin-1/2 Heisenberg models. *Computer Physics Communications* **212** 180-188; DOI: https://doi.org/10.1016/j.cpc.2016.09.003.

[6] D.S. GAUNT, A.J. GUTTMANN (1974) Asymptotic Analysis of Coefficients, Chapter 4. In: C. Domb, M.S. Green (eds) "Phase Transitions and Critical Phenomena", 181-243.

[7] C. DOMB (1971) In: M.S. Green (ed) "Proceedings of the Enrico Fermi Summer School of Physics, Varenna". Academic Press, New York.

[8] A.J. GUTTMANN (1989) Chapter 1: Asymptotic Analysis of Power Series Expansions. In: C. Domb and J. Lebowitz (eds) "Phase Transitions and Critical Phenomena", vol. 13.

[9] C.J. PEARCE (1978) Transformation methods in the analysis of series for critical properties. *Advances in Physics* **27**(1) 89-145 DOI: https://doi.org/10.1080/00018737800101354.

[10] H.E. STANLEY (1967) High-Temperature Expansions for the Classical Heisenberg Model. II. Zero-Field Susceptibility. *Physical Review* **158**(1) 546-553; DOI: https://doi.org/10.1103/PhysRev.158.546.

[11] C. DOMB, M.F. SYKES (1956) On Metastable Approximations in Co-Operative Assemblies. *Proceedings of the Royal Society A* **235**(1201) 247-259 DOI: https://doi.org/10.1098/rspa.1956.0080.

[12] Й. БРАНКОВ, К. КРЕЖОВ (1980) Анализ высокотемпературного ряда методом оптимального преобразования. *Сообщения ОИЯИ*, P17-80-551, 1-11.

[13] K. KREJOV, S. BIDIKOV, J. BRANKOV, B. SIDJIMOV (1980) High-temperature susceptibilities for a type of Heisenberg model magnetics. *Bulgarian Journal of Physics* **7**(1) 95-115.

[14] H.D. HUNTER, G.A. BAKER (1973) Methods of series analysis. I. Comparison of Current Methods used in the Theory of Critical Phenomena. *Physical Review B* **7**(6) 3346-3376; DOI: https://doi.org/10.1103/PhysRevB.7.3346.

[15] K. KREJOV, S. BIDIKOV, J. BRANKOV, B. SIDJIMOV (1980) Evidence from high temperature susceptibilities of the Heisenberg model ferrimagnet $RbNiF_3$. *Journal of Physics C: Solid State Physics* **13** article no 20, pp. 5413-5422; DOI: https://doi.org/10.1088/0022-3719/13/29/020.

[16] K. KREZHOV, J. BRANKOV (1981) Optimal Transformation Method of Analysis of High-Temperature Expansion of Susceptibility for Heisenberg RbNiF3 Ferrimagnet (High temperature series expansion analysis of susceptibility of the Heisenberg ferrimagnet RbNiF3). *Физика Твердого Тела* **23**(8) 2820-2826.

[17] S. BIDIKOV, K. KREJOV (1980) High-Temperature Specific Heat for a Type of Heisenberg Model Magnetics. *Bulgarian Journal of Physics* **7**(1) 183-189.

[18] J.A. KAFALAS, M. LONGO (1968) Effect of pressure on the structure and magnetic properties of RbNiF3. *Materials Research Bulletin* **3**(5) 501-506; DOI: https://doi.org/10.1016/0025-5408(68)90074-3.

[19] V. ANTONOV, K. KREZHOV, N. TRENDAFILOVA (2010) First principles study of electronic and crystallographic structure and elastic properties of $RbNiF_3$, 7th General Conference of Balkan Physical Union, BPU-7, 9-13 September, 2009, Alexandroupolis, Greece, *AIP Conference Proceedings* **1203** (1) – Jan 21, 2010, pp. 1143-1148; DOI: http://www.aip.org/proceedings.

[20] J. WEIDENBORNER, A. BEDNOWITZ (1970) Structures of ferrimagnetic fluorides of ABF3 type. I. RbNiF3. *Acta Crystallographica B* **26**(9) 1464-1468; DOI: https://doi.org/10.1107/S0567740870004338.

[21] J. ALS-NIELSEN, R.G. BIRGENEAU, .J. GUGGENHEIM (1972) Neutron-Scattering Study of Spin Waves in the Ferrimagnet RbNiF3. *Physical Review B* **6**(4) 2030-2039; DOI: https://doi.org/10.1103/PhysRevB.6.2030.

[22] S. PICKART, H. ALPERIN (1968) Magnetic Structure of RbNiF3. *Journal of Applied Physics* **39** 1332-4; DOI: https://doi.org/10.1063/1.1656286.

[23] S. PICKART, H. ALPERIN (1971) Magnetic Structures of Ferrimagnetic $RbNiF_3$ and $CsFeF_3$. *Journal of Applied Physics* **42** 1617-19. DOI: https://doi.org/10.1063/1.1660365.

[24] K. KREZHOV, P. KONSTANTINOV (2000) Neutron Diffraction Investigation of $RbNiF_3$. In: R. Delhez, E.J. Mittemeijer (eds) "Materials Science Forum" **321-324** pp. 938-941; DOI: https://doi.org/10.4028/www.scientific.net/MSF.321-324.938.

[25] K. KREZHOV (2004) Low temperature neutron diffraction study of $RbNiF_3$. *Journal of Magnetism and Magnetic Materials* **272–276** (Part 2) 845-847; DOI: https://doi.org/10.1016/j.jmmm.2003.11.354.

[26] R.V. PISAREV, J. FERRE, R.H. PETIT, B.B. KRICHEVTSOV, P.P. SYRNIKOV (1974) Magneto-optical study of the 3A2 to 1Ea transition in magnetic crystals KNiF3, Rb2NiF4, K3Ni2F7, RbNiF3. *Journal of Physics C: Solid State Physics* **7**(22) 4143; DOI: https://doi.org/10.1088/0022-3719/7/22/019.

[27] G.A. SMOLESKII, V.M. YUDIN, P.P. SYRIKOV, A.B. SHERRNAN (1966) *Fiz. Tverd. Tela* **8** 2965-9; (translation G.A. Smolensky, V.M. Yudin, P.P. Syrnikov, A.B. Sherman (1967) Sov. Phys. Solid St. **8** 2368-71); (1966)

[28] .W. SHAFER, .R. MCGUIRE, B.. ARGYLE, G.J. FAN (1967) Magnetic and optical properties of transparent $RbNiF_3$. *Applied Physics Letters* **10**(6) 202-4; DOI: https://doi.org/10.1063/1.1754911.

[29] S.R. CHINN, .J. ZEIGER, J.R. O'CONNOR (1971) Two-Magnon Raman Scattering and Exchange Interactions in Antiferromagnetic $KNiF_3$ and K_2NiF_4 and Ferrimagnetic $RbNiF_3$. *Physical Review B* **3**(4) 1709-1735; DOI: https://doi.org/10.1103/PhysRevB.3.1709.

[30] G. PAUL, H.E. STANLEY (1972) Partial Test of the Universality Hypothesis: The Case of Different Coupling Strengths in Different Lattice Directions. *Physical Review B* **5**(6) 2578-99; DOI: https://doi.org/10.1103/PhysRevB.5.2578.

[31] M.P. PETROV, V.V. MOSKALEV, G.A. SMOLENSKYI (1970) Stimulated ferromagnetism and the effects of short range magnetic ordering in RbNiF3. *Solid State Communications* **8**(2) 157-160; DOI: https://doi.org/10.1016/0038-1098(70)90069-4.